Exploring the Vibrational Fingerprint of the Electronic Excitation Energy via Molecular Dynamics — Supplementary Material

Andy Van Yperen-De Deyne,[1] Thierry De Meyer,[1] Ewald Pauwels,[1, a)] An Ghysels,[1] Karen De Clerck,[2] Michel Waroquier,[1] Veronique Van Speybroeck,[1] and Karen Hemelsoet[1, b)]

[1)] *Center for Molecular Modeling (CMM), Ghent University, Technologiepark 903, 9052 Zwijnaarde, Belgium*

[2)] *Department of Textiles, Ghent University, Technologiepark 907, 9052 Zwijnaarde, Belgium*

(Dated: 7 March 2014)

[a)] Current address: UGent HPC, Ghent University, Krijgslaan 281, S9, B-9000 Gent

[b)] Electronic mail: karen.hemelsoet@ugent.be

a. Ethylene The occurrence of mixing modes - representative of the Duschinsky effect - should correspond to peaks at $\omega_i + \omega_j$ and $|\omega_i - \omega_j|$.[1]. Mixing of modes 4 (torsion) and 10 (CC stretch) implies frequency peaks at 4096 and 2038 cm^{-1}. Due to the complication of possible overlap with other peaks in the region slightly above 2000 cm^{-1}, we concentrate on the high frequency peak at 4096 cm^{-1}. This peak is indeed observable in Figure S1. All peaks in the region above 2100 cm^{-1} have very low intensities. For example, the intensity of the peak at 4096 cm^{-1} is only 0.1 % of those in Figure 5a.

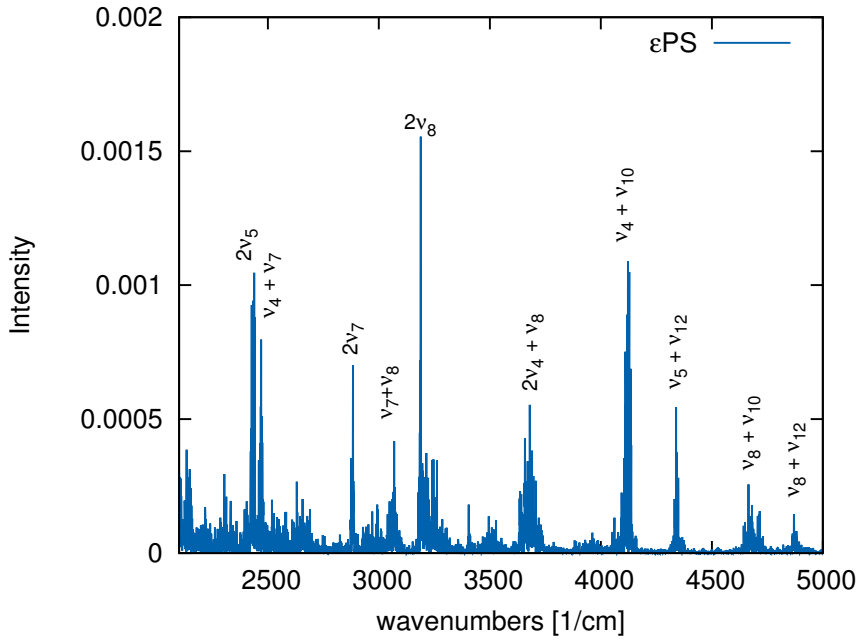

FIG. S1: The high frequency range of the ϵPS of ethylene. The peaks are labeled by the combinations at the appropriate position. In order of increasing frequency the following assignments can be made: $2\nu_5$ =2422 cm^{-1}, $\nu_4 + \nu_7$ = 2469 cm^{-1}, $2\nu_7$ = 2882 cm^{-1}, ν_{10} = 3067 cm^{-1}, $2\nu_8$ = 3187 − 3336 cm^{-1}, $2\nu_4 + \nu_8$ = 3680 cm^{-1}, $\nu_4 + \nu_{10}$ =4096 cm^{-1}, $\nu_5 + \nu_{12}$ =4336 cm−1, $\nu_8 + \nu_{10}$ =4667 cm^{-1}, $\nu_8 + \nu_{12}$ = 4872 cm^{-1}.

b. Biphenyl Detailed overview of the results for the $S_0 \rightarrow T_1$ transition of biphenyl (MD at 600 K) are given. Figure S2 displays the ϵPS compared with the overall VPS. Due to the complexity of the VPS, it is difficult to determine linearly or quadratically active peaks and therefore Q_iPS are used instead.

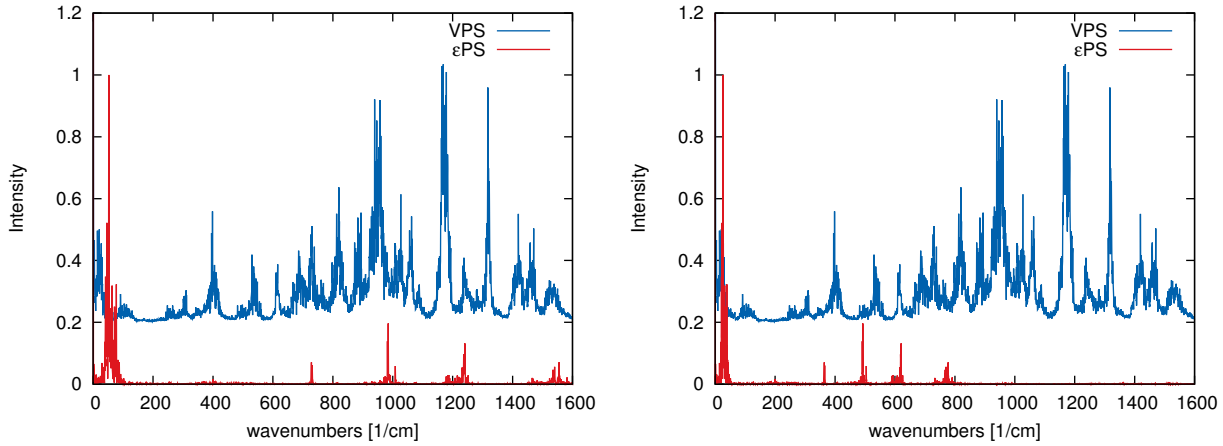

(a) (b)

FIG. S2: (a) Calculated VPS (blue, shifted upwards) and ϵPS (red) for biphenyl. (b) The VPS (blue, shifted upwards) and scaled ϵPS (red) for biphenyl.

Overall, 7 Q_iPS spectra were found that exhibit peaks that coincide with characteristic peaks in the ϵPS: 5 linearly active (see Figure S3) and 2 quadratically active (see Figure S4).

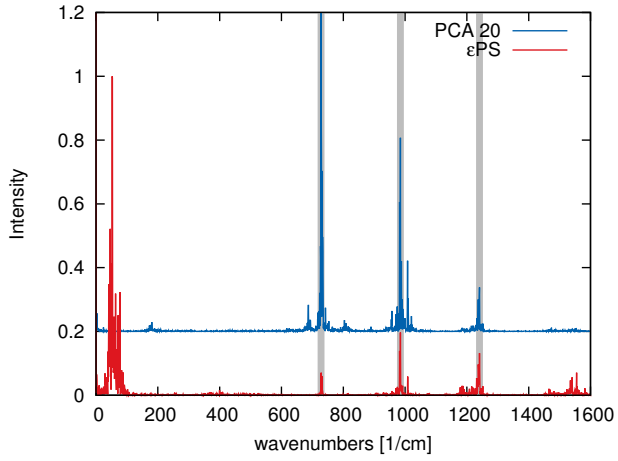

(a)

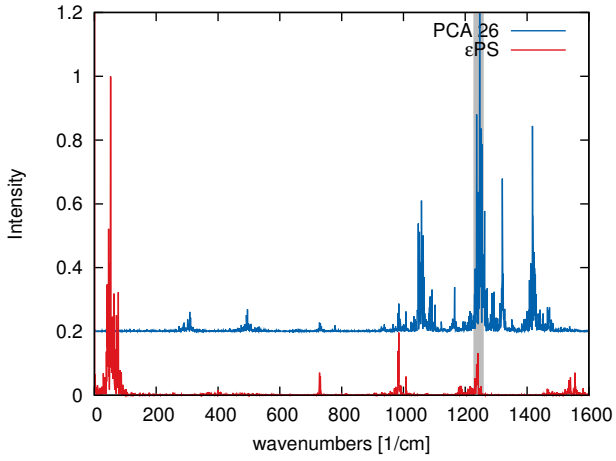

(b)

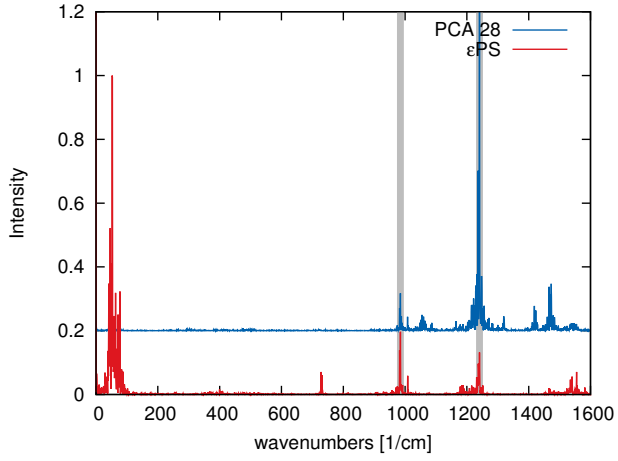

(c)

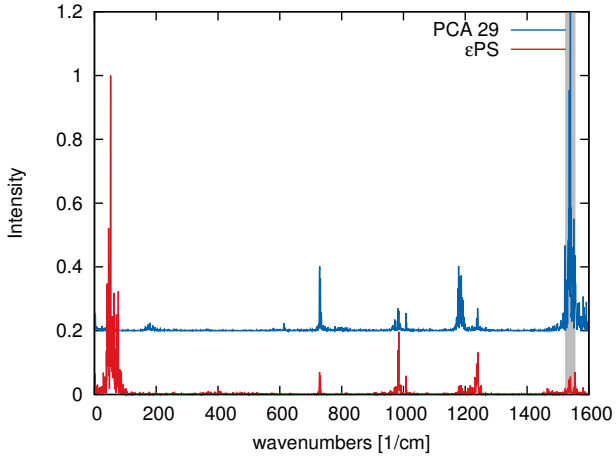

(d)

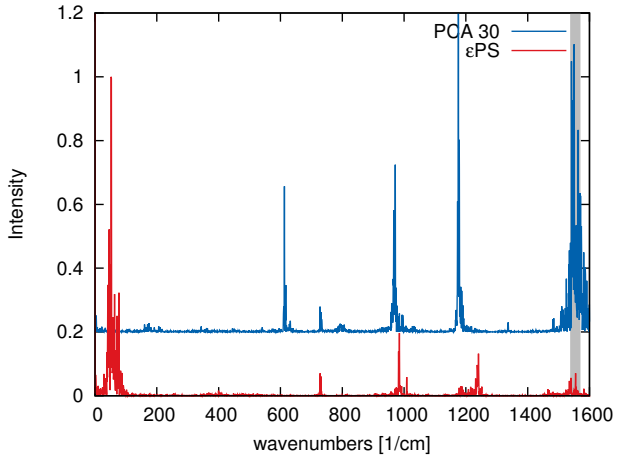

(e)

FIG. S3: Calculated Q_iPS (blue, shifted upwards) and ϵPS (red) for biphenyl. Five linearly active modes can be distinguished: Q_{20}, Q_{26}, Q_{28}, Q_{29} and Q_{30}.

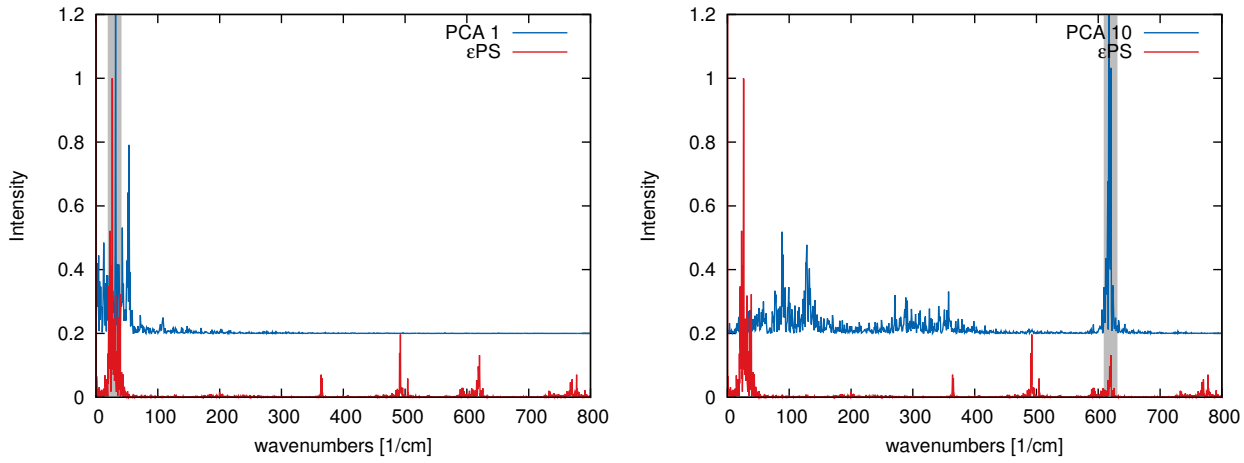

(a) (b)

FIG. S4: Calculated $Q_i PS$ (blue, shifted upwards) and scaled ϵPS (red) for biphenyl. Two quadratically active modes can be distinguished: Q_1 and Q_{10}.

c. Ethyl orange in gas phase A more detailed assignment of the peaks of ϵ_1PS and ϵ_2PS is given in Figures S5 and S6. In both ϵPS spectra, four peaks can be distinguished; two are observed (at 860 and 1051 cm^{-1}) in both power spectra. In the case of ethyl orange, no clear quadratic mode is identified; although they might be present but with much lower intensities.

Figure S5 shows that the first excitation energy (ϵ_1 in the main text) changes mostly with C-N-N scissors (mode Q_{33}), azo N-N stretch (mode Q_{40} and Q_{47}) and related C-N stretches (mode Q_{47} and Q_{51}). It is no surprise these are influencing the HOMO-1 orbital (see Figure 10a in the main manuscript), since it is located at the azo bond. Note that both Q_{47} and Q_{33} do not perfectly correspond to isolated peaks in their power spectrum. Comparing with other power spectra of principal components resulted in a very plausible assignment.

In contrast to the HOMO-1, the HOMO orbital is a π-like orbital spread over both phenyl groups and therefore ring vibrations are dominating the ϵ_2PS (Figure S6). These are located at 1052 cm^{-1} (Q_{54}) and three peaks at 1330 cm^{-1} (Q_{60}), both corresponding to in plane ring vibrations. Surprisingly, the out-of-plane motions as well as global motions (such as a phenyl-azo-phenyl bending motion) are not or less pronounced in the ϵ_2PS. The N-N stretch is again present in the ϵ_2PS but much less dominant compared to the ϵ_1PS. Both Q_{47} and Q_{51} can be correlated to this power spectrum.

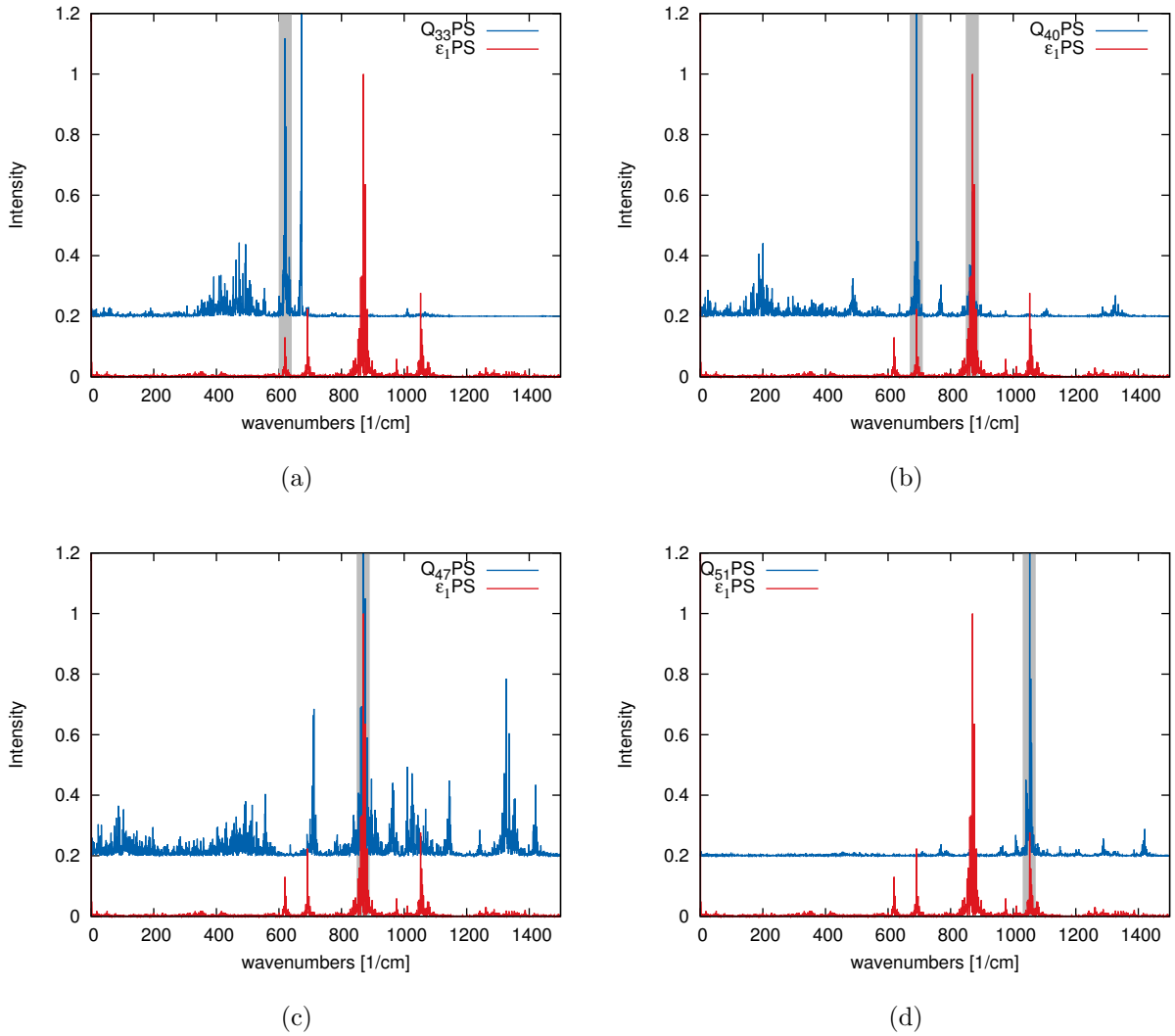

FIG. S5: Assignment of peaks in the ϵ_1PS to principal components Q_i via the Q_iPS. (a) Q_{33} with peak position at 620 cm^{-1}, corresponding with a C-N-N scissor motion (b) Q_{40} with peak positions at both 690 cm^{-1} and 869 cm^{-1} and (c) Q_{47} located at mainly 869 cm^{-1} both corresponding to N-N stretching motions, (d) Q_{51} with peak position at 1052 cm^{-1} corresponding with C-N stretches.

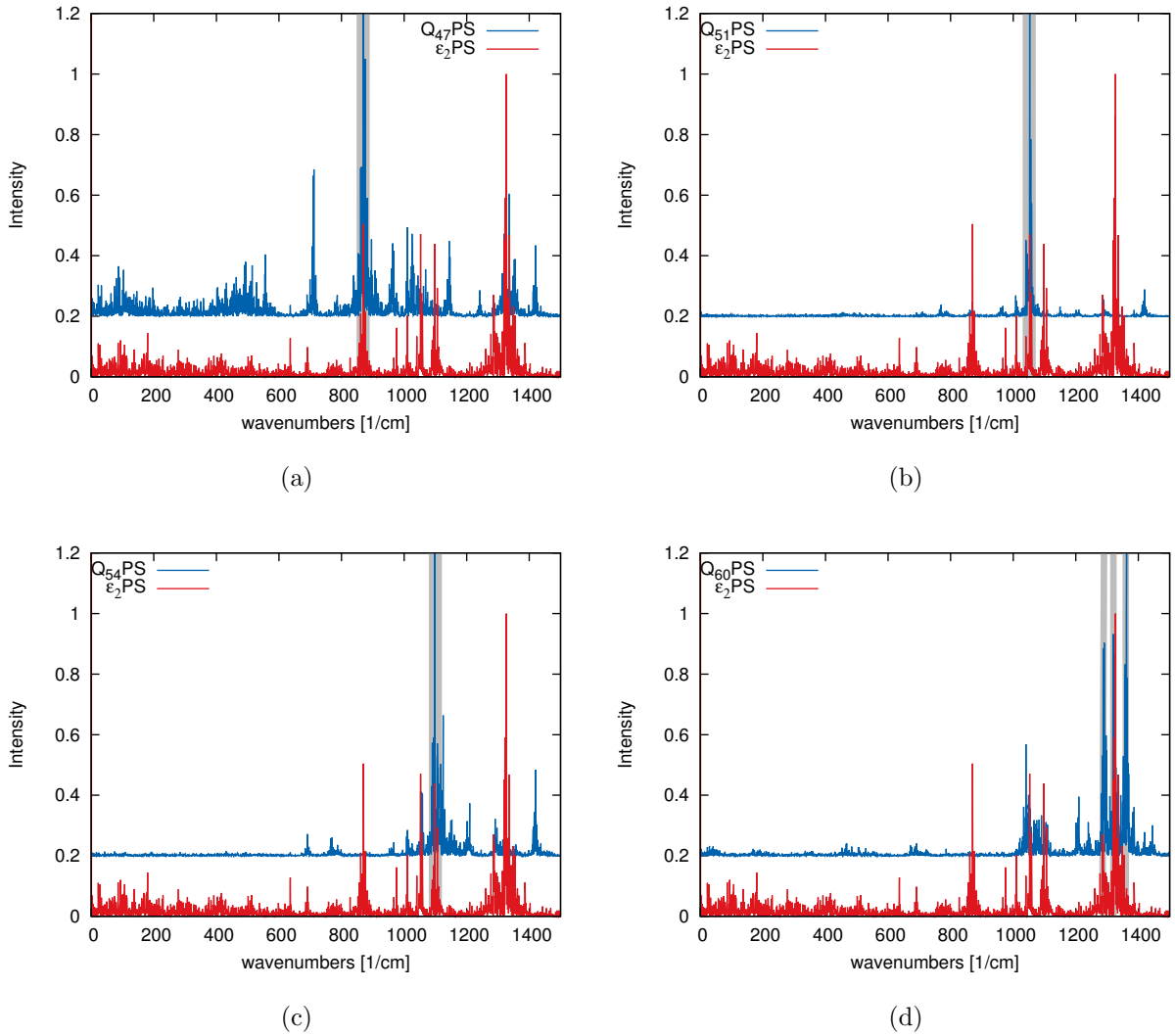

(a) (b)

(c) (d)

FIG. S6: Assignment of peaks in the ϵ_2PS to principal components Q_i via the Q_iPS. (a) Q_{47} corresponding to a N-N stretch at 869 cm^{-1}, (b) Q_{51} at 1052 cm^{-1} related to the C-N stretch in azo-benzene, (c) Q_{54} located at 1100 cm^{-1} and (d) Q_{60} located at 1330 cm^{-1}, both corresponding to in-plane ring vibrations.

d. Influence of water on ethyl orange When an explicit solvent, treated at the MM level, is added during the MD simulation, a dynamic spectrum (using snapshots from the QM/MM MD run followed by TD-DFT simulations on the isolated dye) can be computed which is in excellent agreement with an experimentally measured UV/Vis spectrum of the solvated dye as shown in Figure S7.

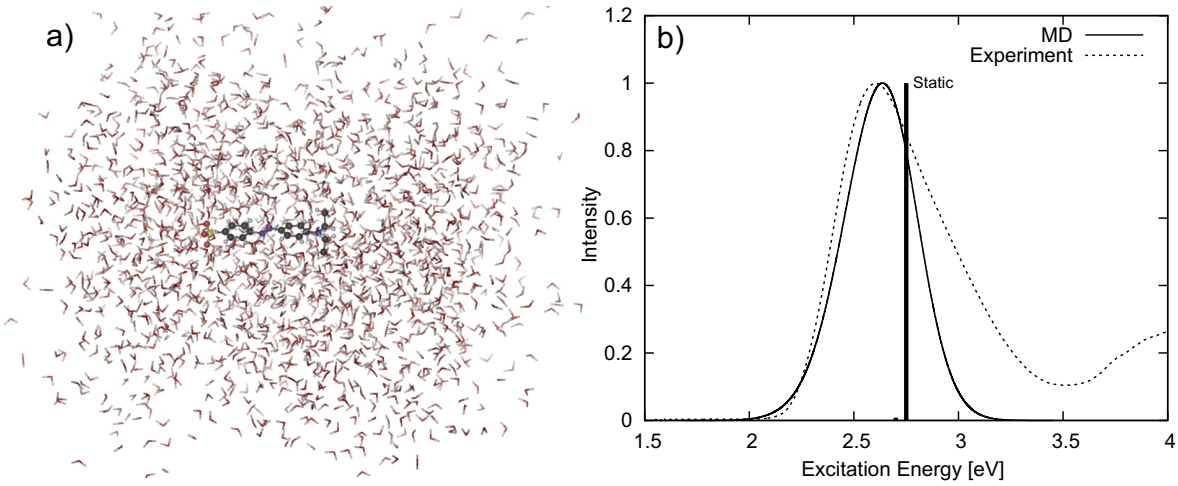

FIG. S7: (a) Ethyl orange surrounded by a water box containing 1830 water molecules used for the QM/MM MD simulation. (b) Experimental and computed MD UV/Vis spectra. The static vertical excitation energies (both the first and second excitation) - corresponding with the optimized structure of ethyl orange in a PCM surrounding - are also given.

However, the power spectra resulting from the original QM/MM MD simulation are much more noisier and interpretation is less convenient. Additional peaks in the power spectra are clearly present (see Figure S8), e.g. below 500 cm^{-1} several peaks are present for ϵ_2PS in the case of the solvated molecule. A clear assignment of these new peaks is not feasible with PCA and therefore other methods should be used. This lies beyond the scope of this work.

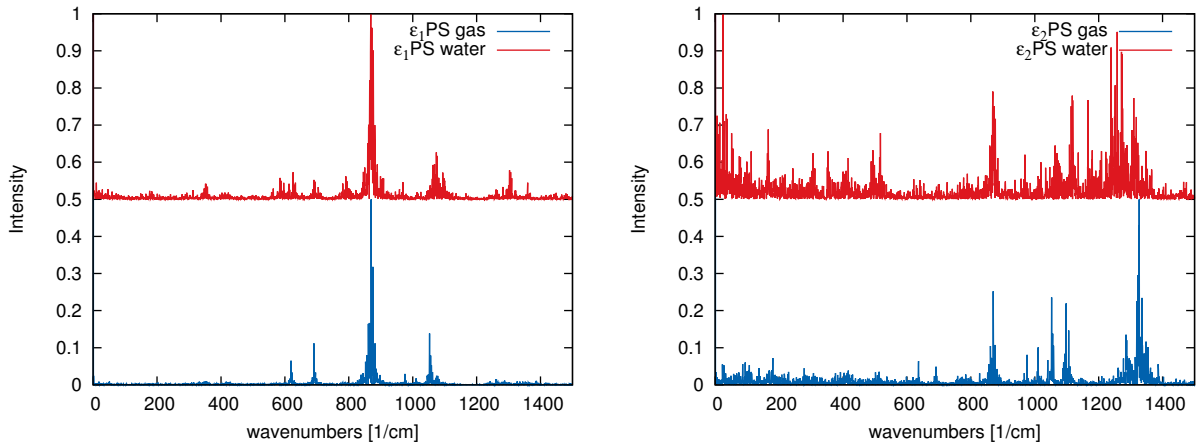

(a) (b)

FIG. S8: The ϵ_1PS and ϵ_2PS for gas phase case (blue) and the solvated case (red).

e. Ethyl orange for $\epsilon_1 < \epsilon_2$ at each time step When for each time step the smallest excitation energy is considered to be ϵ_1 and the second ϵ_2, different excitations are monitored within the same signal. This can clearly be seen in Figures S9a,b: the oscillator strength is crossing at almost each sampled step. The resulting ϵPS contains more noise and peaks at positions related to this level crossing rather then the actual change of a particular situation (see Figure S9c). The main characteristics are preserved (e.g. high intensity at 869 cm^{-1}), but new peaks are introduced in the ϵ_1PS which correspond to phenyl ring vibrations, proven not to be as dominant for the HOMO-1 to LUMO transition.

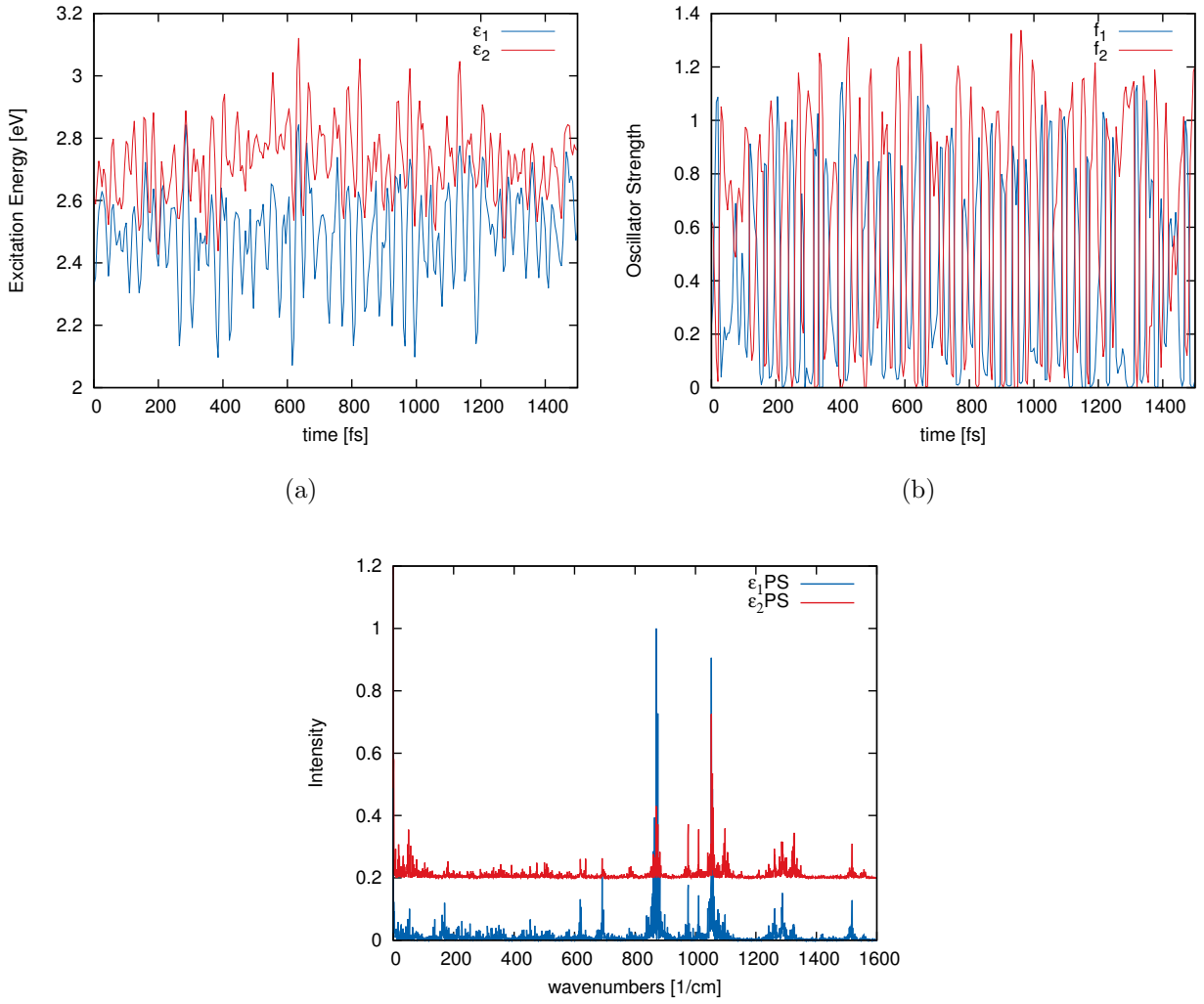

(a) (b)

(c)

FIG. S9: (a) Excitation trajectory for the first 1.5 ps, (b) Trajectory of the oscillator strength, (c) The resulting ϵ_1PS and ϵ_2PS when level crossing is not taken into account.

REFERENCES

[1]A. M. Mebel, Y. T. Chen, and S. H. Lin, Chem. Phys. Lett. **258**, 53 (1996).